ARTICLE

doi:10.1038/nature11656

Zero-valent sulphur is a key intermediate in marine methane oxidation

Jana Milucka[1], Timothy G. Ferdelman[1], Lubos Polerecky[1], Daniela Franzke[1], Gunter Wegener[1,2], Markus Schmid[3], Ingo Lieberwirth[4], Michael Wagner[3], Friedrich Widdel[1] & Marcel M. M. Kuypers[1]

Emissions of methane, a potent greenhouse gas, from marine sediments are controlled by anaerobic oxidation of methane coupled primarily to sulphate reduction (AOM). Sulphate-coupled AOM is believed to be mediated by a consortium of methanotrophic archaea (ANME) and sulphate-reducing Deltaproteobacteria but the underlying mechanism has not yet been resolved. Here we show that zero-valent sulphur compounds (S^0) are formed during AOM through a new pathway for dissimilatory sulphate reduction performed by the methanotrophic archaea. Hence, AOM might not be an obligate syntrophic process but may be carried out by the ANME alone. Furthermore, we show that the produced S^0—in the form of disulphide—is disproportionated by the Deltaproteobacteria associated with the ANME. Our observations expand the diversity of known microbially mediated sulphur transformations and have significant implications for our understanding of the biogeochemical carbon and sulphur cycles.

Anaerobic oxidation of methane coupled to sulphate reduction (AOM), according to equation (1), has a crucial role in the carbon and sulphur cycling in marine environments.

$$CH_{4(aq)} + SO_4^{2-} \rightarrow HS^- + HCO_3^- + H_2O \quad \Delta G = -34\,kJ\,mol^{-1}\ CH_4 \quad (1)$$

At most investigated AOM sites and in sulphate-reducing enrichment cultures, anaerobic methanotrophic archaea (ANME; groups ANME-1, -2 and -3) and Deltaproteobacteria have been found to co-occur[1]. Therefore, it has been proposed that the two organisms mediate AOM, presumably in a syntrophic manner[2–4], and thus share the extremely low energy yield of the net reaction (equation (1)). However, the biological basis for AOM has persistently eluded clarification and remains a geomicrobiological puzzle[5].

We have obtained through continuous cultivation over 8 years a highly enriched AOM culture from sediments of the Mediterranean mud volcano Isis, which is particularly suitable for physiological investigations. As shown by catalysed reporter deposition fluorescence *in situ* hybridization (CARD-FISH), the large and irregularly-shaped ANME-2 and their smaller, rod- to vibrio-shaped partner bacteria (*Desulfosarcina/Desulfococcus* cluster; DSS) together account for up to 95% of all cells[6]. The culture grows by oxidation of methane, the sole added organic carbon substrate, to CO_2 with concomitant reduction of sulphate to sulphide (Fig. 1a, b). Single-cell analyses by nanometre-scale secondary ion mass spectrometry (nanoSIMS) show that both microbial groups primarily (>90% of cellular C) derive their biomass carbon from dissolved inorganic carbon (DIC) assimilation and have similar doubling times of 130–160 days (Supplementary Table 1). These values are in agreement with the doubling times deduced previously from bulk measurements in AOM enrichment cultures[7,8]. The preferential assimilation of DIC by DSS bacteria indicates that these organisms are lithoautotrophs[8], and do not directly assimilate methane. ANME assimilate both methane-derived and inorganic carbon (Supplementary Table 1).

Immunodetection of canonical sulphate-reducing enzymes (ATP sulphurylase (Sat) and dissimilatory sulphite reductase (Dsr)) and methyl-coenzyme M reductase (Mcr; an archaeal enzyme involved in methane oxidation) in the two abundant cell populations (Fig. 1c) is

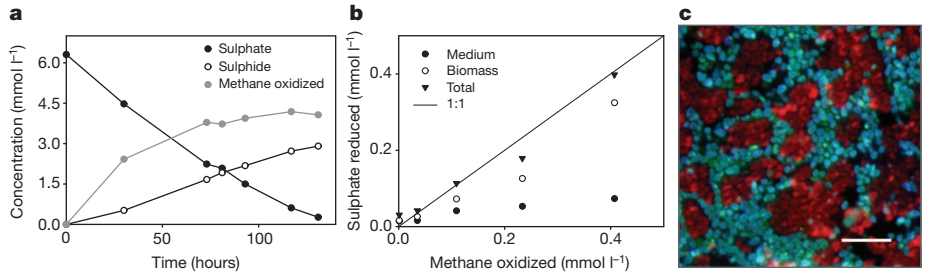

Figure 1 | Microbial activity and composition of the Isis enrichment culture. **a**, Anaerobic oxidation of methane determined from $^{13}CO_2$ production, decrease in sulphate concentration and increase in sulphide concentration versus time (hours) in incubations with added $^{13}CH_4$ ($n = 3$). **b**, Total sulphate-derived reduced sulphur species (a sum of reduced sulphur in medium and reduced sulphur in biomass) as determined from ^{35}S accumulation versus methane oxidation as determined from $^{14}CO_2$ production in incubations with added [^{35}S]sulphate and $^{14}CH_4$ during the first 11 h of a batch incubation ($n = 1$; this experiment was repeated twice). **c**, AOM aggregate labelled with anti-Sat (ATP sulphurylase, green), anti-Dsr (dissimilatory sulphite reductase, blue) and anti-Mcr (methyl-CoM reductase, red) antibodies. Mcr is localized in the larger, irregularly shaped ANME-2 (red), whereas Sat and Dsr co-localize in the rod-shaped DSS bacteria (turquoise). Scale bar, 5 μm.

[1]Max Planck Institute for Marine Microbiology, Celsiusstrasse 1, 28359 Bremen, Germany. [2]Alfred Wegener Institute, Am Handelshafen 12, 27570 Bremerhaven, Germany. [3]University of Vienna, Althanstrasse 14, A-1090 Vienna, Austria. [4]Max Planck Institute for Polymer Research, Ackermannweg 10, 55128 Mainz, Germany.

consistent with the hypothesis that, in AOM consortia, methane oxidation and (canonical) dissimilatory sulphate reduction are catalysed by ANME and DSS bacteria, respectively. Moreover, the high abundance of DSS bacteria and their similar doubling times with the ANME serve as a support for involvement of both organisms in AOM. Several hypotheses propose a syntrophic mechanism of these consortia, all of which assume a flow of electrons from the ANME to the bacteria. Available experimental evidence[9,10] as well as most current modelling studies[11–13], however, show that putative syntrophic intermediates (that is, hydrogen, formate, acetate or methanol) are not used as electron donors for sulphate reduction during AOM. Other theories suggest a role for methanethiol[14], use of extracellular nanowires[15,16] or a direct cell-to-cell contact for direct electron transfer. Yet evidence for these hypotheses is still lacking.

Zero-valent sulphur as an intermediate

If the syntrophy is based on extracellular diffusion of a chemical compound, this is expected to be formed from the substrate or from a compound readily available in the environment. We therefore considered involvement of sulphur in oxidation states other than the abundant sulphate or sulphide as a syntrophic intermediate in AOM. Zero-valent sulphur (S^0), in the form of elemental sulphur and dissolved polysulphide sulphur, is commonly measured in the highly reducing, sulphidic environments that characterize AOM ecosystems[17], indicating that not all sulphate is reduced to the –II oxidation state. As the reduction of one sulphate to S^0 only requires six of the eight electrons obtained from methane oxidation, the measured sulphate reduction rates determined from decrease in sulphate would exceed those of anaerobic oxidation of methane. This would result in AOM and sulphate reduction rates that are not coupled exactly in the 1:1 stoichiometry given by equation (1)[18,19]. Interestingly, in our enrichment culture less sulphide was produced than expected from the decrease in sulphate (Fig. 1a), indicating that reduced sulphur other than sulphide is formed during AOM-coupled sulphate reduction.

The presence of S^0 in wet biomass of our AOM enrichment culture was confirmed by anaerobic extraction with methanol and subsequent analysis of S_8 by high-performance liquid chromatography (HPLC), which revealed elemental sulphur content of up to approximately 5 mmol S per gram of dry biomass (~15% w/w). Wet biomass was also anaerobically extracted in the presence of methyl trifluoromethanesulphonate, a strong methylating agent that prevents oxidation of labile polysulphides into elemental sulphur by converting them into stable dimethylpolysulphides, which are HPLC- and gas-chromatography-amendable[20]. HPLC analysis of the methyl trifluoromethanesulphonate-treated methanol extracts showed that the sample contained, besides colloidal sulphur, substantial (up to 0.5 mmol l^{-1}) amounts of all measurable inorganic polysulphides (S_3^{2-} to S_8^{2-}; Supplementary Fig. 1). The presence of polysulphides in the AOM biomass was confirmed by gas chromatography-mass spectrometry. In contrast, biomass-free medium from the same active culture contained little to no detectable S^0.

By using confocal micro-Raman spectroscopy with approximately 1 μm resolution we detected elemental sulphur in ANME cells identified by FISH (Fig. 2a and Supplementary Fig. 2a–c). Characteristic and strong Raman peaks for elemental sulphur[21,22] were also recorded in untreated ANME cells (Supplementary Fig. 2d), indicating intracellular accumulation of substantial amounts of elemental sulphur in living cells. NanoSIMS analyses of fixed and sectioned cells showed that ANME cells (Fig. 2b–e), identified by antibodies against Mcr (Fig. 2e), have substantially higher sulphur content than DSS cells (~30% higher $^{32}S/^{12}C$ ratio on average, Supplementary Fig. 3). Although the ANME and the DSS are present in equal abundance (for example, Fig. 1c), most of the AOM biomass is composed of ANME (~75%) due to their substantially larger size (ANME/DSS volume ratio = 3:1; Fig. 2b, c). Therefore, we assume that the bulk of the intracellular S^0 in the biomass is present in the ANME cells. Interestingly, the sulphur content of the ANME correlated ($R^2 = 0.8$; $P < 0.0001$) with the rate of methane assimilation (and thus methane oxidation; Fig. 2f and Supplementary Fig. 4), indicating

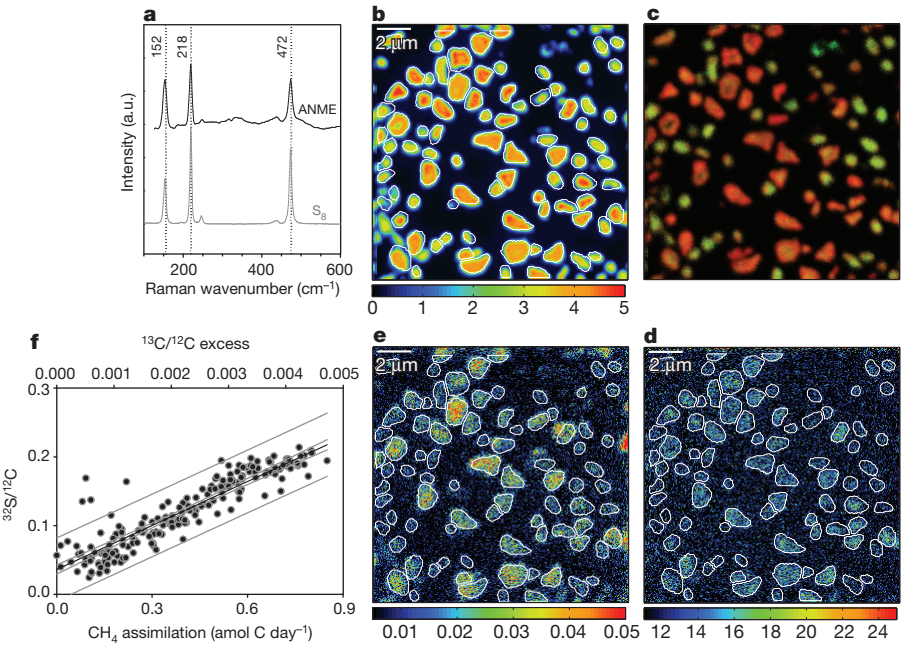

Figure 2 | Zero-valent S in ANME cells in the Isis enrichment culture. **a**, Representative Raman spectrum of an ANME cell, identified by FISH ($n = 1$; 30 additional ANME-2 spectra were measured; see also Supplementary Fig. 2), containing prominent peaks at 152, 218 and 472 cm^{-1} characteristic for elemental sulphur (see our reference spectrum of S_8 and refs 21 and 22). a.u., Arbitrary units. **b**–**e**, NanoSIMS images of Isis enrichment aggregates incubated with ^{13}C-labelled methane. **b**, Individual cells in an AOM aggregate visualized by $^{12}C^{14}N/^{12}C$ ion image. **c**, Composite image showing sulphur-rich ANME cells (red) and phosphorus-rich DSS cells (green), raw data for this image are provided in Supplementary Fig. 13. **d**, $^{13}CH_4$-derived ^{13}C assimilation by ANME shown by a $^{13}C/^{12}C$ image (values were multiplied by 1,000). **e**, $^{197}Au/^{12}C$ image showing ANME cells targeted by gold-labelled antibodies against Mcr. Coloured scale below panels **b**, **d** and **e** shows ratio of the respective ions. **f**, $^{13}C/^{12}C$ excess and the respective methane assimilation determined from $^{13}CH_4$-incubations versus $^{32}S/^{12}C$ ratio for ANME cells ($n = 198$). Scale bars, 2 μm.

that intracellular sulphur in the ANME cells is turned over in relation to AOM.

To identify the source of the S^0, our enrichment culture was incubated under AOM conditions for up to 24 h with $^{34}SO_4^{2-}$ and $^{35}SO_4^{2-}$. The accumulation of sulphate-derived reduced sulphur species in the medium and in the biomass was followed over time. In incubations with a small (<50 μmol l^{-1}) added non-labelled sulphide pool, ^{35}S-label from sulphate was detectable in the AOM biomass within 1 h and preceded the release of detectable [^{35}S]sulphide into the medium (Supplementary Fig. 5). It is unlikely that the biomass S is a result of assimilatory metabolism because the rate of sulphur accumulation (μmol to mmol per litre per day) by far exceeds the sulphur requirements of these ultra-slow-growing organisms (pmol to nmol per litre per day). Moreover, the rate of sulphur accumulation exceeds the rate of carbon assimilation by the ANME by two orders of magnitude, indicating that the sulphur present in ANME biomass is not used for growth (Supplementary Fig. 6). The rates of overall sulphur turnover (calculated as a sum of both biomass sulphur and reduced sulphur in the medium) were proportional to the measured methane oxidation rates (Fig. 1b). Moreover, the total amount of sulphate reduced (that is, biomass sulphur and sulphide) and methane oxidized approximately follows the 1:1 ratio predicted from the overall stoichiometry of the AOM reaction (equation (1)). This agrees well with the approximately 1:1 ratio for methane oxidation coupled to sulphate reduction previously reported for this and other sulphate-reducing AOM enrichment cultures (for example, refs 10 and 23).

Accumulation of ^{35}S label from sulphate in the AOM biomass before its appearance in the sulphide pool strongly indicates that sulphide oxidation is not the source of biomass sulphur. Indeed, our enrichment culture is maintained under strongly reducing conditions, with no detectable potential oxidants for sulphide other than sulphate. Moreover, incubation of the culture in the presence of [^{35}S]sulphide did not lead to a sustainable increase in the ^{35}S content of the biomass with time (Supplementary Fig. 7) as observed during the [^{35}S]sulphate addition experiment (Supplementary Fig. 5). This shows that the accumulation of $^{35}S^0$ in the biomass is neither a result of isotope exchange, nor sulphide oxidation, but rather results directly from the reduction of [^{35}S]sulphate (Supplementary Discussion). To the best of our knowledge, this is the first evidence for direct S^0 formation during sulphate reduction. Our results indicate that zero-valent sulphur formation in strongly reducing environments can occur even when no potential oxidants other than sulphate (for example, Fe III-containing minerals) are available.

Archaeal sulphate reduction

The AOM-dependent accumulation and turnover of sulphate-derived S^0 in the ANME leads us to conclude that ANME are capable of reducing sulphate to S^0 and, potentially, to sulphide. Accordingly, the addition of bacterial inhibitors (tetracycline and streptomycin) had no detectable effect on the rate of sulphate reduction in the enrichment culture (Supplementary Fig. 8). The enzymatic mechanism of this archaeal sulphate reduction is unclear. All genes and proteins for dissimilatory sulphate reduction that have been so far retrieved from AOM environments and cultures have been shown to be of bacterial origin (for example, refs 6 and 24). Protein immunodetection showed that the ANME did not contain detectable amounts of the canonical enzymes for sulphate reduction (for example, Fig. 1c). Therefore, we propose that sulphate reduction in the ANME might proceed via an enzymatic pathway other than the canonical one (that is, involving Sat, Apr and Dsr). Notably, the formylmethanofuran (MFR)/CO_2 + MFR redox couple in methanotrophic archaea has a sufficiently low standard midpoint potential (−530 mV) to serve as an electron donor for direct reduction of sulphate to sulphite without the use of ATP[25], which is needed to activate sulphate in all known dissimilatory sulphate-reducing microorganisms. Although experimental evidence for such mechanism is not yet available, this could explain why the non-thermophilic archaeal sulphate reduction has so far remained undetected despite being proposed numerous times[26–30].

Bacterial disulphide disproportionation

Direct coupling of methane oxidation to dissimilatory sulphate reduction in the ANME indicates that we must reconsider the role of the Deltaproteobacteria in AOM. The abundant expression of Sat and Dsr enzymes by the DSS in our enrichment culture (Fig. 1c) does not necessarily mean that they perform canonical sulphate reduction. Other pathways, such as sulphide oxidation and disproportionation of intermediate oxidation state sulphur compounds (elemental sulphur, thiosulphate and sulphite), also use Sat, Apr and Dsr[31,32]. Our incubation experiments with ^{35}S-labelled sulphide render sulphide oxidation unlikely (Supplementary Fig. 7). To test whether the DSS have the capacity to disproportionate, we added colloidal sulphur (approximately 7 mmol l^{-1}) to the Isis enrichment culture in the absence of methane or any other electron donors. Immediately, linear production of sulphide and sulphate was observed (Supplementary Fig. 9) that reached a stoichiometric ratio of 7:1 (Fig. 3a) that was maintained until all added sulphur was consumed. The stoichiometric ratio for elemental sulphur disproportionation is 3:1, significantly lower than the 7:1 ratio observed in our experiment, but under sulphidic conditions that prevail in our incubations, elemental sulphur would react with dissolved sulphide to form soluble inorganic polysulphides that can also be disproportionated. Indeed, the theoretical ratio of sulphide to sulphate production during disulphide disproportionation is exactly 7:1 (equation (2), Supplementary Table 2)

$$4HS_2^- + 4H_2O \rightarrow SO_4^{2-} + 7HS^- + 5H^+ \quad \Delta G = -12.7\ \mathrm{kJ\ mol^{-1}}\ HS_2^- \quad (2)$$

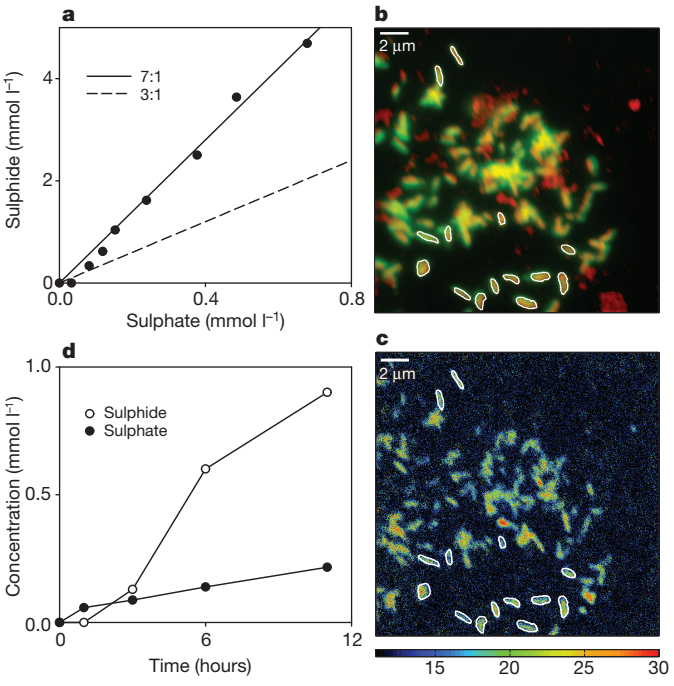

Figure 3 | Disulphide disproportionation by Isis enrichment culture. **a**, Linear correlation between sulphate and sulphide production in the Isis enrichment culture incubated with $^{13}CO_2$ and colloidal sulphur in the absence of methane over the course of 70 days ($n = 1$) follows the 7:1 ratio inferred for disulphide disproportionation. **b**, Overlay of nanoSIMS $^{12}C^{14}N$ image (red) and fluorescence image of microorganisms from the enrichment culture stained with the DSS-658 probe (green). **c**, The $^{13}C/^{12}C$ image shows that the DSS cells (several of which are shown by white outlines) are enriched in ^{13}C. Coloured scale below panel **c** shows ratio of the respective ions. **d**, Production of sulphide and sulphate (based on ^{35}S accumulation in sulphate after the addition of ^{35}S-sulphide) under AOM conditions ($n = 1$; this experiment was repeated twice).

indicating that the organisms in our AOM enrichment disproportionate this most simple of all inorganic polysulphides. The rates of disulphide disproportionation remained constant over a wide range of sulphide concentrations (at least 5 mmol l^{-1}), indicating that disproportionation of disulphide is less sensitive to sulphide than disproportionation of elemental sulphur, and can thus occur in sulphidic environments. To confirm that disulphide disproportionation can support growth, autotrophic carbon assimilation in the biomass was followed by the addition of $H^{14}CO_3^-$ and $H^{13}CO_3^-$ to the medium. The amount of ^{14}C in the bulk AOM biomass increased with time (Supplementary Fig. 9), indicating that the observed disproportionation is coupled to energy generation and growth. Indeed, single-cell nanoSIMS analysis revealed that DSS-class Deltaproteobacteria, identified by CARD-FISH, were capable of autotrophic growth under disproportionating conditions (Fig. 3b, c). Interestingly, ANME-2 were no longer detectable in the enrichment culture after 70 days of incubation in the presence of colloidal sulphur (Supplementary Fig. 10).

The evidence that disulphide disproportionation also occurs under AOM conditions was provided by the $H^{35}S^-$-addition experiment. A substantial part of the ^{35}S from ^{35}S-labelled sulphide was recovered in the sulphate pool, although no net sulphate production was observed (Fig. 3d and Supplementary Fig. 11). The rates of sulphide production to tracer-derived sulphate production were approximately 6:1, similar to the 7:1 ratio observed during disulphide disproportionation. In a comparable experiment with the same culture[23], a ratio of produced sulphide to sulphate of approximately 8:1 was obtained. Our combined results indicate that the high transfer rate of [^{35}S]sulphide to the sulphate pool (~12% of AOM rate) can be primarily attributed to the disproportionation of disulphide or S^0.

Model for sulphate-dependent AOM

On the basis of our observations and thermodynamic considerations, we propose the following model for sulphur cycling between ANME-2 and Deltaproteobacteria involved in AOM (Fig. 4). ANME-2 perform anaerobic oxidation of methane and reduction of sulphate to disulphide (or another S^0 compound, and possibly partly even all the way to sulphide). Disulphide is taken up by the DSS and disproportionated to sulphide and sulphate in a 7:1 ratio. Sulphate formed during disproportionation is partly re-used by the ANME-2 to oxidize methane and thus no net sulphate production occurs. The overall stoichiometry of AOM coupled to disproportionation (one mole sulphate reduced per one mole methane oxidized) remains 1:1 (that is, sum of equations (2) and (3) gives equation (1)).

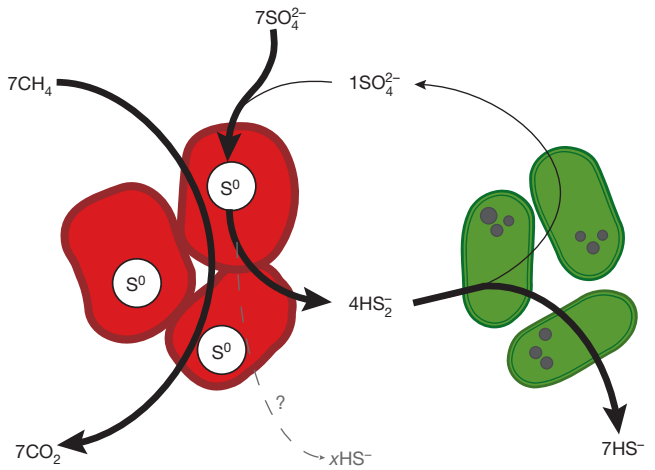

Figure 4 | Revised model of anaerobic oxidation of methane coupled to sulphate reduction. ANME-2 oxidize methane with a concomitant reduction of sulphate to zero-valent sulphur (S^0, elemental sulphur) that is partially deposited or bound intracellularly. Produced S^0 is exported or diffuses outside the cell where it reacts with sulphide to form polysulphides (disulphide, among others). Disulphide is taken up by the associated Deltaproteobacteria and is disproportionated to sulphate and sulphide. Sulphate produced during disproportionation might be re-used by the ANME and the ANME may also reduce some of the sulphate all the way to sulphide (grey dotted line). Dark circles in the bacteria represent intracellular precipitates rich in iron and phosphorus (Fig. 2c and Supplementary Fig. 14).

$$4HS_2^- + 4H_2O \rightarrow SO_4^{2-} + 7HS^- + 5H^+ \quad \Delta G = -12.7\ \text{kJ mol}^{-1}\ HS_2^- \quad (2)$$

$$7CH_{4(aq)} + 8SO_4^{2-} + 5H^+ \rightarrow 4HS_2^- + 7HCO_3^- + 11H_2O \quad \Delta G = -26.5\ \text{kJ mol}^{-1}\ CH_4 \quad (3)$$

Thermodynamic calculations show that the energy gain of the ANME is greater than that of the DSS, which could explain why the ANME-2:DSS cell abundance ratio in our cultures is maintained close to 1:1 while their size and presumably also biomass ratio is 3:1.

Although the phylogenetically distinct ANME-1 and -3 clusters may have different physiologies, our model could explain the occurrence of single active ANME-2 cells in *in vitro* incubations[33] and in marine environments[30,34]. The ANME-2 might not depend directly on the activity of bacterial partners because in environments rich in sulphate and methane, sulphate reduction to disulphide is exergonic over a wide range of disulphide concentrations (Supplementary Fig. 12 and Supplementary Discussion). Interestingly, disulphide in its partly protonated form (HS_2^-) is particularly stable at around neutral pH and low Eh[35], conditions typical for AOM zones. Although disulphide has largely eluded detection in natural environments, it should be abundant in marine sediments that are undersaturated with respect to S^0 (ref. 17). Thermodynamic calculations also show that AOM coupled to sulphate reduction becomes energetically more favourable if the disulphide produced is scavenged (Supplementary Fig. 12). In principle, ANME-2 can associate with any bacteria that possess the capacity to scavenge the disulphide produced. In several studies ANME-2 and -3 were found to co-exist with bacteria of the order Desulfobulbaceae[36–38]. Notably, bacteria belonging to this order have been shown to be capable of disproportionation[39,40]. Thus, a model whereby archaea reduce sulphate to zero-valent sulphur while mediating methane oxidation, and the bacteria gain energy from disproportionation, is consistent with known distributions of archaea and bacteria in AOM habitats.

Biogeochemical implications

Our model could also explain why sulphate reduction has been detected in deeply-buried, methane- and sulphide-rich sediments[41] inhabited by archaea[42,43]. The deep subsurface is dominated by a large number of different archaeal groups such as the miscellaneous crenarchaeotal group[44] and marine benthic group B that lack cultured representatives and whose physiology is largely unexplored. It is possible that these archaea might have also adopted a unique pathway for sulphate reduction that might not be necessarily coupled to methanotrophy. The revised model for AOM (Fig. 4), by necessity, should lead to a re-evaluation of the biogeochemistry of methane oxidation and sulphur cycling in marine environments. Current diagenetic models for deep marine sediments are deficient, or 'leaky' with respect to their redox balance[45]. Although methane is oxidized to CO_2 (8 e^-), the ultimate end-product of sulphate reduction in deep marine sediments takes the form of buried iron disulphide, pyrite, in which S has an oxidation state of –I. Archaeal sulphate reduction to S^0 provides a source of zero-valent sulphur for the formation of pyrite and would therefore mitigate the need to provide an external oxidant (for example, Fe III; ref. 46).

Overall, to our knowledge our observations provide for the first time strong evidence that intercellular sulphur cycling occurs between ANME-2 and DSS Deltaproteobacteria during AOM, which involves new pathways of sulphate reduction and disulphide disproportionation.

These results also greatly expand the range of conditions under which sulphur disproportionation is likely to occur[47], and, in a large picture, encourage the re-evaluation of the role of sulphate-reducing archaea and sulphur-disproportionating bacteria in present-day and early Earth environments.

METHODS SUMMARY

In all AOM experiments, the Isis enrichment culture was incubated anaerobically in artificial seawater medium with methane as sole electron donor and sulphate as sole electron acceptor. To determine the potential for S^0 disproportionation, colloidal sulphur was added to the medium and the culture was incubated without methane and sulphate.

Methane oxidation rates were determined from $^{13}CO_2$ production in $^{13}CH_4$ incubations by gas chromatography-isotope ratio mass spectrometry or from $^{14}CO_2$ production in $^{14}CH_4$ incubations by scintillation counting. Sulphate reduction rates were determined as changes in sulphate and sulphide concentrations determined by ion chromatography and photometrically, respectively, and from [^{35}S]sulphide production in [^{35}S]sulphate incubations. Sulphate production was determined by ion chromatography in the disproportionation experiments. The sulphate production under AOM conditions was determined from [^{35}S]sulphate production in [^{35}S]sulphide incubations. Elemental S and polysulphide concentrations in biomass and medium were determined by liquid chromatography.

Microbial aggregates from the AOM experiments were collected for immunolabelling, fixed with formaldehyde and cryosectioned. Subsequently, the sections were labelled with primary antibodies targeting either key enzyme(s) for anaerobic oxidation of methane (Mcr) or the canonical sulphate reduction pathway (Apr and Dsr) and fluorochrome- or gold-coupled secondary antibodies. Samples from the disproportionation experiment were collected for halogen *in situ* hybridization. Assimilation of [^{13}C]DIC and [^{14}C]DIC in the biomass in the various experiments was followed by bulk ^{13}C measurements, with nanometre-scale secondary ion mass spectrometry (nanoSIMS) and by scintillation counting, respectively. Doubling times and carbon assimilation of single cells were determined from [^{13}C]methane or [^{13}C]DIC incubations by using nanoSIMS. The presence of S^0 in single cells was determined by Raman-FISH.

Thermodynamic calculations were made for the concentrations and activity coefficients typical for the start of a batch enrichment culture and are listed in Supplementary Information (Supplementary Tables 3, 4 and 5).

Full Methods and any associated references are available in the online version of the paper.

Received 12 April; accepted 3 October 2012.
Published online 7 November 2012.

1. Knittel, K. & Boetius, A. Anaerobic oxidation of methane: progress with an unknown process. *Annu. Rev. Microbiol.* **63,** 311–334 (2009).
2. Hoehler, T. M., Alperin, M. J., Albert, D. B. & Martens, C. S. Field and laboratory studies of methane oxidation in an anoxic marine sediment: evidence for a methanogen-sulfate reducer consortium. *Glob. Biogeochem. Cycles* **8,** 451–463 (1994).
3. Boetius, A. *et al.* A marine microbial consortium apparently mediating anaerobic oxidation of methane. *Nature* **407,** 623–626 (2000).
4. Orphan, V. J., House, C. H., Hinrichs, K. U., McKeegan, K. D. & DeLong, E. F. Methane-consuming archaea revealed by directly coupled isotopic and phylogenetic analysis. *Science* **293,** 484–487 (2001).
5. Alperin, M. & Hoehler, T. The ongoing mystery of sea-floor methane. *Science* **329,** 288–289 (2010).
6. Schreiber, L., Holler, T., Knittel, K., Meyerdierks, A. & Amann, R. Identification of the dominant sulfate-reducing bacterial partner of anaerobic methanotrophs of the ANME-2 clade. *Environ. Microbiol.* **12,** 2327–2340 (2010).
7. Nauhaus, K., Albrecht, M., Elvert, M., Boetius, A. & Widdel, F. *In vitro* cell growth of marine archaeal-bacterial consortia during anaerobic oxidation of methane with sulfate. *Environ. Microbiol.* **9,** 187–196 (2007).
8. Wegener, G., Niemann, H., Elvert, M., Hinrichs, K. U. & Boetius, A. Assimilation of methane and inorganic carbon by microbial communities mediating the anaerobic oxidation of methane. *Environ. Microbiol.* **10,** 2287–2298 (2008).
9. Meulepas, R. J. W., Jagersma, C. G., Khadem, A. F., Stams, A. J. M. & Lens, P. N. L. Effect of methanogenic substrates on anaerobic oxidation of methane and sulfate reduction by an anaerobic methanotrophic enrichment. *Appl. Microbiol. Biotechnol.* **87,** 1499–1506 (2010).
10. Nauhaus, K., Boetius, A., Kruger, M. & Widdel, F. *In vitro* demonstration of anaerobic oxidation of methane coupled to sulphate reduction in sediment from a marine gas hydrate area. *Environ. Microbiol.* **4,** 296–305 (2002).
11. Sørensen, K. B., Finster, K. & Ramsing, N. B. Thermodynamic and kinetic requirements in anaerobic methane oxidizing consortia exclude hydrogen, acetate, and methanol as possible electron shuttles. *Microb. Ecol.* **42,** 1–10 (2001).
12. Orcutt, B. & Meile, C. Constraints on mechanisms and rates of anaerobic oxidation of methane by microbial consortia: process-based modeling of ANME-2 archaea and sulfate reducing bacteria interactions. *Biogeosciences* **5,** 1587–1599 (2008).
13. Alperin, M. J. & Hoehler, T. M. Anaerobic methane oxidation by archaea/sulfate-reducing bacteria aggregates: 1. Thermodynamic and physical constraints. *Am. J. Sci.* **309,** 869–957 (2009).
14. Moran, J. J. *et al.* Methyl sulfides as intermediates in the anaerobic oxidation of methane. *Environ. Microbiol.* **10,** 162–173 (2008).
15. Meyerdierks, A. *et al.* Metagenome and mRNA expression analyses of anaerobic methanotrophic archaea of the ANME-1 group. *Environ. Microbiol.* **12,** 422–439 (2010).
16. Shima, S. & Thauer, R. K. Methyl-coenzyme M reductase and the anaerobic oxidation of methane in methanotrophic Archaea. *Curr. Opin. Microbiol.* **8,** 643–648 (2005).
17. Holmkvist, L. *et al.* Sulfate reduction below the sulfate-methane transition in Black Sea sediments. *Deep Sea Res. Part I Oceanogr. Res. Pap.* **58,** 493–504 (2011).
18. Joye, S. B. *et al.* The anaerobic oxidation of methane and sulfate reduction in sediments from Gulf of Mexico cold seeps. *Chem. Geol.* **205,** 219–238 (2004).
19. Hansen, L. B., Finster, K., Fossing, H. & Iversen, N. Anaerobic methane oxidation in sulfate depleted sediments: effects of sulfate and molybdate additions. *Aquat. Microb. Ecol.* **14,** 195–204 (1998).
20. Kamyshny, A., Ekeltchik, I., Gun, J. & Lev, O. Method for the determination of inorganic polysulfide distribution in aquatic systems. *Anal. Chem.* **78,** 2631–2639 (2006).
21. Pasteris, J. D., Freeman, J. J., Goffredi, S. K. & Buck, K. R. Raman spectroscopic and laser scanning confocal microscopic analysis of sulfur in living sulfur-precipitating marine bacteria. *Chem. Geol.* **180,** 3–18 (2001).
22. Trofimov, B. A., Sinegovskaya, L. M. & Gusarova, N. K. Vibrations of the S-S bond in elemental sulfur and organic polysulfides: a structural guide. *J. Sulfur Chem.* **30,** 518–554 (2009).
23. Holler, T. *et al.* Carbon and sulfur back flux during anaerobic microbial oxidation of methane and coupled sulfate reduction. *Proc. Natl Acad. Sci. USA* **108,** E1484–E1490 (2011).
24. Basen, M. *et al.* Bacterial enzymes for dissimilatory sulfate reduction in a marine microbial mat (Black Sea) mediating anaerobic oxidation of methane. *Environ. Microbiol.* **13,** 1370–1379 (2011).
25. Thauer, R. K. Biochemistry of methanogenesis: a tribute to Marjory Stephenson. *Microbiology* **144,** 2377–2406 (1998).
26. Widdel, F., Musat, F., Knittel, K. & Galushko, A. in *Sulphate-Reducing Bacteria: Environmental and Engineered Systems* (eds Barton, L. *et al.*) 265–303 (Cambridge Univ. Press, 2007).
27. Johnson, E. F. & Mukhopadhyay, B. in *Microbial Sulfur Metabolism*. (eds Dahl, C. *et al.*) 202–216 (Springer, 2008).
28. Thauer, R. K. & Shima, S. in *Incredible Anaerobes: from Physiology to Genomics to Fuels* Vol. 1125 158–170 (Wiley-Blackwell, 2008).
29. Thauer, R. K. Anaerobic oxidation of methane with sulfate: on the reversibility of the reactions that are catalyzed by enzymes also involved in methanogenesis from CO_2. *Curr. Opin. Microbiol.* **14,** 292–299 (2011).
30. Orphan, V. J., House, C. H., Hinrichs, K. U., McKeegan, K. D. & DeLong, E. F. Multiple archaeal groups mediate methane oxidation in anoxic cold seep sediments. *Proc. Natl Acad. Sci. USA* **99,** 7663–7668 (2002).
31. Krämer, M. & Cypionka, H. Sulfate formation via ATP sulfurylase in thiosulfate-disproportionating and sulfite-disproportionating bacteria. *Arch. Microbiol.* **151,** 232–237 (1989).
32. Trüper, H. G. & Fischer, U. Anaerobic oxidation of sulfur compounds as electron donors for bacterial photosynthesis. *Phil. Trans. R. Soc. Lond. B* **298,** 529–542 (1982).
33. House, C. H., Beal, E. J. & Orphan, V. J. The apparent involvement of ANMEs in mineral dependent methane oxidation, as an analog for possible Martian methanotrophy. *Life* **1,** 19–33 (2011).
34. Treude, T. *et al.* Consumption of methane and CO_2 by methanotrophic microbial mats from gas seeps of the anoxic Black Sea. *Appl. Environ. Microbiol.* **73,** 2271–2283 (2007).
35. Rickard, D. & Luther, G. W. Chemistry of iron sulfides. *Chem. Rev.* **107,** 514–562 (2007).
36. Niemann, H. *et al.* Novel microbial communities of the Haakon Mosby mud volcano and their role as a methane sink. *Nature* **443,** 854–858 (2006).
37. Lösekann, T. *et al.* Diversity and abundance of aerobic and anaerobic methane oxidizers at the Haakon Mosby mud volcano, Barents Sea. *Appl. Environ. Microbiol.* **73,** 3348–3362 (2007).
38. Pernthaler, A. *et al.* Diverse syntrophic partnerships from deep-sea methane vents revealed by direct cell capture and metagenomics. *Proc. Natl Acad. Sci. USA* **105,** 7052–7057 (2008).
39. Lovley, D. R. & Phillips, E. J. P. Novel processes for anaerobic sulfate production from elemental sulfur by sulfate-reducing bacteria. *Appl. Environ. Microbiol.* **60,** 2394–2399 (1994).
40. Fuseler, K. & Cypionka, H. Elemental sulfur as an intermediate of sulfide oxidation with oxygen by *Desulfobulbus propionicus*. *Arch. Microbiol.* **164,** 104–109 (1995).
41. Parkes, R. J. *et al.* Deep sub-seafloor prokaryotes stimulated at interfaces over geological time. *Nature* **436,** 390–394 (2005).
42. Lipp, J. S., Morono, Y., Inagaki, F. & Hinrichs, K. U. Significant contribution of Archaea to extant biomass in marine subsurface sediments. *Nature* **454,** 991–994 (2008).
43. Teske, A. & Sørensen, K. B. Uncultured archaea in deep marine subsurface sediments: have we caught them all? *ISME J.* **2,** 3–18 (2008).
44. Kubo, K. *et al.* Archaea of the Miscellaneous Crenarchaeotal Group are abundant, diverse and widespread in marine sediments. *ISME J.* **6,** 1949–1965 (2012).

45. Meysman, F. J. R. & Middelburg, J. J. Acid-volatile sulfide (AVS) — a comment. *Mar. Chem.* **97,** 206–212 (2005).
46. Holmkvist, L., Ferdelman, T. G. & Jørgensen, B. B. A cryptic sulfur cycle driven by iron in the methane zone of marine sediment (Aarhus Bay, Denmark). *Geochim. Cosmochim. Acta* **75,** 3581–3599 (2011).
47. Philippot, P. *et al.* Early Archaean microorganisms preferred elemental sulfur, not sulfate. *Science* **317,** 1534–1537 (2007).

Supplementary Information is available in the online version of the paper.

Acknowledgements We want to thank G. Klockgether, K. Imhoff, S. Littmann and T. Vagner for technical support, G. Lavik and M. Formolo for analytical support and discussions, M. Schüler and T. Keil for assistance with cryosectioning, A. Boetius for providing samples, and T. Holler for the initial enrichment and maintenance of the Isis culture. This work was financially supported by the Max Planck Society and the ERC Advanced Grant 294343 (to M.W.).

Author Contributions J.M., T.G.F., F.W. and M.M.M.K. designed experiments. J.M., T.G.F. and M.M.M.K. performed experiments and analysed data. J.M. performed immunolabeling and microscopy. D.F. performed CARD-FISH and nanoSIMS. L.P. analysed nanoSIMS data. M.S. and M.W. performed Raman measurements, I.L. performed energy-dispersive X-ray spectroscopy analyses, and G.W. contributed new analytical tools. J.M., T.G.F. and M.M.M.K. wrote the manuscript with contributions of all co-authors.

Author Information Reprints and permissions information is available at www.nature.com/reprints. The authors declare no competing financial interests. Readers are welcome to comment on the online version of the paper. Correspondence and requests for materials should be addressed to J.M. (jmilucka@mpi-bremen.de).

METHODS

Cultivation and incubation experiments. The enrichment culture 'Isis' was obtained through continuous (>8 years) incubation from a sediment sample collected on a cruise of RV *L'Atalante* in September 2003 in the eastern Mediterranean Sea (depth ~990 m, *in situ* temperature ~14 °C[50]). The culture was incubated in artificial seawater medium (pH 7.5; salt composition: 0.76 mmol l^{-1} KBr, 8.05 mmol l^{-1} KCl, 10 mmol l^{-1} $CaCl_2 \cdot 2H_2O$, 27.9 mmol l^{-1} $MgCl_2 \cdot 6H_2O$, 27.6 mmol l^{-1} $MgSO_4 \cdot 7H_2O$, 451 mmol l^{-1} NaCl, 4.67 mmol l^{-1} NH_4Cl, 1.47 mmol l^{-1} KH_2PO_4; buffer: 30 mmol l^{-1} HCO_3^-; trace elements and vitamins prepared and added according to ref. 51; reducing agent ~0.5 mmol l^{-1} Na_2S) in closed culture vials with CH_4:N_2:CO_2 (75:22.5:2.5) headspace. Methane (Air Liquide) was added to 3 bar overpressure unless indicated otherwise. AOM activity was followed by quantification of methane-dependent sulphide formation using spectrophotometry[52]. When sulphide concentrations in the medium reached ~10 mmol l^{-1} used medium was replaced by fresh medium. All experiments were performed at room temperature and during all incubations the vials were continuously shaken (40 r.p.m.) to facilitate gas transport.

Maintenance and handling of the culture was performed in an anoxic glove box (Mecaplex) under N_2:CO_2 (90:10) atmosphere. For all experiments an active preculture with high AOM rates (0.24 mmol HS^- per gram (dry weight) per day) was used but the culture was diluted into aliquots with different activities for individual experiments.

For the inhibition experiments with selected antibiotics, active Isis culture was aliquoted into three 70 ml serum bottles (25 ml medium + biomass and 45 ml headspace) and pre-incubated for 72 h under AOM conditions (3 bar CH_4 overpressure, ~30 atom % ^{13}C; ISOTEC, Sigma-Aldrich) until linear sulphide production was observed. Then, without releasing methane overpressure, streptomycin and tetracycline were added (anoxically and in sterile conditions) to two of the serum bottles, respectively, from a sterile anoxic stock solution (5 g l^{-1} each) to a final concentration of 25 mg l^{-1}. This concentration has been reported to have inhibitory effect on sulphate-reducing bacteria[53]. The third bottle was untreated with antibiotics and served as a control. The bottles were incubated on a shaker (40 r.p.m.) at room temperature in the dark. Subsamples were taken anoxically with needles at regular time intervals to monitor the methane oxidation as well as changes in the concentration of total sulphate and sulphide. The sampling involved following: 0.3 ml culture was filtered through a 0.2-μm filter into 50% $ZnCl_2$ for sulphide measurements, 0.3 ml culture was filtered through a 0.2-μm filter into 0.01 M HCl for sulphate measurements and 0.5 ml culture was filtered onto a 0.22-μm GTTP filter for ^{35}S-scintillation counting. Sulphide was measured using colorimetry[54], sulphate was measured as described below. Methane oxidation rates were calculated from the measured production of $^{13}CO_2$. For $^{13}CO_2$ measurements, 1 ml of sample was filtered through a 0.22-μm filter into a sterile Exetainer. The headspace of the Exetainer was then exchanged with Helium and the sample was acidified by the addition of 100 μl 85% phosphoric acid through the Exetainer septum. The samples were stored upside down at room temperature until measured with gas chromatography-isotope ratio mass spectrometry (GC-IRMS; Fisons VG Optima).

To test for the disproportionation potential of the AOM culture, colloidal sulphur, prepared according to ref. 55, was cleaned through repeated cycles (8–10×) of peptization. To bring it into the anoxic glove box, we precipitated ('salted out') the sol one last time with a saturated NaCl solution and removed the supernatant. In the glove box the pelleted colloid was brought back into solution in sulphate-free artificial seawater medium. Sulphate-free artificial seawater medium was prepared as described above with following modifications: trace elements solution did not contain $FeSO_4 \cdot 7H_2O$, $MgSO_4 \cdot 7H_2O$ was replaced by $MgCl_2 \cdot 6H_2O$ (55.5 mmol l^{-1} final concentration), and NaCl concentration was changed correspondingly to 423 mmol l^{-1}. Then, active AOM culture (washed with sulphate-free artificial seawater medium) was added to the bottle containing medium with colloidal sulphur. The final sulphur concentration in the incubation was approximately 8 mmol l^{-1}. The culture (in a 118 ml serum bottle; 50 ml medium + biomass and 68 ml headspace) was then supplemented with ^{13}C-bicarbonate (~5 mmol l^{-1}; ISOTEC, Sigma-Aldrich) and ^{14}C-bicarbonate (10 MBq; Hartmann Analytics) and the pH of the medium was adjusted with 4 M HCl to 7.5. The culture was incubated with an N_2:CO_2 headspace (no added methane, no overpressure) on a shaker (40 r.p.m.) in the dark. During first 70 days, subsamples were regularly taken to monitor sulphate and sulphide production and ^{14}C-incorporation into biomass. The sampling involved following: 0.4 ml culture was filtered through a 0.2-μm filter into 50% $ZnCl_2$ for sulphide measurements, 0.3 ml culture was filtered through a 0.2-μm filter into 0.01 M HCl for sulphate measurements, and 0.5 ml culture was filtered onto a 0.22-μm GTTP filter for ^{14}C-scintillation counting. Sulphide was measured using colorimetry[54], sulphate was measured as described below. The ^{14}C content of the biomass was determined by filtering an aliquot of the culture onto a 0.22-μm filter, washing it with 20 ml sterile anoxic artificial seawater medium and twice with 20 ml 1 M HCl. The filters obtained were subsequently decalcified overnight, in a desiccator with fuming 37% HCl. After decalcification the filter was dried and the radioactivity was measured by scintillation counting (scintillation cocktail: PermaFluorTM; scintillation counter: 2900TR LSA, Packard). At each sampling point small (undefined) amounts of biomass were also fixed with 4% formaldehyde for nanoSIMS analyses. These highly enriched consortia with their inherently slow growth were available only in limited quantities and, therefore, only several biomass flocs (that is, no fixed volumes) were collected from each incubation for fixation in formaldehyde. NanoSIMS analyses were performed with samples taken at 70 and 270 days (Fig. 3b, c and Supplementary Fig. 10).

CARD/halogen *in situ* hybridization coupled to laser marking and nanoSIMS. Aliquots of the Isis enrichment culture grown under disproportionating conditions were taken at regular intervals and fixed in 2% (final concentration) formaldehyde in 50 mM phosphate buffer (pH 7.4). CARD/Halogen *in situ* hybridization was performed as described previously[56]. Briefly, the sample was filtered onto a Au/Pd-coated polycarbonate filter and embedded in 0.1% low melting point agarose. To permeabilize cells for hybridization, filtered samples were treated with lysozyme (10 g l^{-1}) for 40 min at 37 °C. Subsequently, the filter was washed with water and pre-hybridized for 30 min at 46 °C in a hybridization buffer (50% formamide). After adding the oligonucleotide probe (50 ng DSS-658 coupled to horseradish peroxidase; Biomers) to the hybridization mixture the filter was hybridized for another 4 h at 46 °C. After hybridization the filter was washed with a pre-heated washing buffer (15 min at 48 °C) and transferred into amplification buffer containing 0.15% H_2O_2 and 20 μg Oregon Green-labelled tyramides. The amplification step was performed for 20 min at 46 °C. The filter was then washed with PBS and stained with DAPI (1 ng ml^{-1}) for 10 min at 4 °C in the dark. After washing with water and drying, small circles (5-mm diameter) were cut out of the filter and placed on support glasses to be viewed in a Laser Microdissection microscope (DM 6000 B, Leica). Individual fields of view containing labelled cells were marked with a laser. Subsequently, the filter was embedded in a mixture of Citifluor/Vectashield and fluorescent images of the individual fields of view were obtained with an epifluorescent microscope (Zeiss AxioPlan Microscope). The cover glass was removed and the filter was briefly washed in 96% ethanol and water and left to dry. The cut-out filter pieces were subsequently mounted into a suitable holder and used for nanoSIMS imaging.

Preparation of cryosections. Immunolabelling and nanoSIMS: the sample was fixed in 2% formaldehyde in 50 mmol l^{-1} phosphate buffer (pH 7.4). Fixation was performed for at least 2 h at room temperature. The sample was then briefly washed with cold phosphate buffer to remove precipitates and salt from the medium and stored in fresh 2% formaldehyde in 50 mM phosphate buffer (pH 7.4) at 4 °C until processed further. Biomass flocs were transferred into 2.3 M sucrose and infiltrated overnight at 4 °C on a rotational shaker. Semi-thin cryosections (300–500 nm) prepared as described previously[57] with a Leica Ultracut EM FCS (Leica Microsystems) and were transferred on poly-L-lysine-coated coverslips in a 1:1 mixture of 2.3 M sucrose:methylcellulose, and dried. The sections were stored at −20 °C until further processing.

Confocal Raman microscopy: Isis biomass was fixed in 4% formaldehyde in 50 mM phosphate buffer, washed with PBS, embedded in OCT compound embedding medium and frozen. Frozen sample was mounted on a metal pin of the Leica CM-3050-S cryotome (Leica Microsystems) and sectioned (2–5 μm thickness). The sections were collected with a brush and placed on a support glass slide to thaw.

Immunolabelling on cryosections. Immunofluorescent labelling: immunolabelling with anti-Mcr, anti-Sat and anti-Dsr antibodies as markers for ANME and DSS, respectively, was performed as described in ref. 58. Briefly, thawed cryosections were washed in PBS and then incubated with primary anti-Mcr (rabbit) and anti-Dsr (guinea-pig) antibodies (at 1:200 dilution). After a wash in PBS + 0.01% Tween the sections were further incubated with the following secondary antibodies: goat anti-rabbit IgG coupled to Cy5 (1:200 dilution; Invitrogen) and goat anti-guinea-pig IgG coupled to rhodamine (1:200 dilution; Santa Cruz Biotechnology). Afterwards the sections were thoroughly washed in PBS + 0.01% Tween and incubated with anti-Sat antibodies, which were pre-conjugated to FITC (fluorescein isothiocyanate; Sigma-Aldrich) according to themanufacturer's instructions. The conjugated anti-Sat-FITC antibody was then used at 1:10 dilution. After final wash in water the sections were embedded in Mowiol/DABCO (1,4-diazobicyclo-[2,2,2]-octane; Sigma; 2% w/v)/DAPI (4′,6′-diamidino-2-phenylindole; Sigma; final concentration 1 μg ml^{-1}) mixture, sealed with nail polish and stored at 4 °C.

Immunogold labelling: immunolabelling with anti-Mcr antibody was performed as follows. Cryosections on glass coverslips were washed by positioning the glass 'section-down' on a drop of PBS. Subsequent incubation and washing steps were performed in the same manner. During incubation and washing steps

great care was taken to keep the glass surface with the sections hydrated to prevent cells from drying which would lead to their detachment from the glass support. Immunolabelling was performed with unlabelled primary antibodies raised against methyl-CoM reductase (described in ref. 58). After incubation with primary antibodies the sections were washed three times with PBS + 0.01% Tween. Subsequently, the sections were incubated with secondary antibodies. These secondary antibodies were double-labelled, carrying a fluorochrome (FITC) and a 1.4 nm cluster of NanoGold (Nanoprobes). This double detection system allowed assessment and verification of the specificity of the antibody binding by fluorescence microscopy before nanoSIMS analysis (see Supplementary Fig. 15a). The primary and secondary antibodies were used at 1:200 and 1:20 dilutions, respectively. For epifluorescence microscopy, at this stage the sections were washed, embedded in Mowiol/DABCO/DAPI mixture, sealed with nail polish and stored at 4 °C. Alternatively, for nanoSIMS analysis the sections were washed in water and afterwards incubated for 10 min in 2% methylcellulose in water. Methylcellulose fills the spaces between individual cells and connects them to the glass support underneath. Excess methylcellulose was carefully adsorbed with a filter paper and the glass slide was left to dry. Methylcellulose is stable in high vacuum and is thus compatible with nanoSIMS analysis. In fact, the methylcellulose coating of the sections was found to be essential for a successful nanoSIMS analysis (see further). When dry, the glass was sputter-coated by a thin (~100 nm) platinum layer to avoid charging during nanoSIMS imaging. For handling reasons the sample was metal-coated after methylcellulose coating (the metal layer tends to displace from glass but sticks to methylcellulose). Subsequently, the round coverslip (10-mm diameter) was placed into the standard sample holder of the CAMECA NanoSIMS 50 instrument and analysed.

Image acquisition and processing. The immunolabelled cryosections and CARD-FISH-labelled cells on filters were examined with a Zeiss AxioCam MRc attached to a Zeiss Axioplan Microscope (Zeiss) equipped with an oil immersion planapochromat lens (×100 1.3 numerical aperture; Zeiss). The appropriate filter sets for DAPI, FITC/fluorescein, Cy3/rhodamine and Cy5 were used. The exposure times were <20 ms for DAPI and <300 ms for FITC, rhodamine and Cy5, respectively. The images obtained were processed with Adobe Photoshop.

Combination of fluorescence *in situ* hybridization (FISH) and Raman spectroscopy. Biomass (1 ml) of the Isis enrichment was collected through the septum of an anoxic Hungate tube with a hypodermic needle (Sterican, size 1, 0.90 × 40 mm, B. Braun Melsungen AG) connected to a 1 ml syringe (Injekt-F, B. Braun Melsungen AG). Subsequently, the culture was homogenized by shearing it 10 times through the syringe. Then the biomass was centrifuged, the supernatant was removed and the samples were incubated with 1 ml of 0.01 mmol l^{-1} HCl for 3 h at room temperature to reduce autofluorescence. HCl was removed after another centrifugation step (10,000*g*, 5 min) and the biomass was resuspended in 1 ml 50% ethanol in phosphate buffered saline (PBS; 10 mmol l^{-1} sodium phosphate buffer pH 7.4, 130 m mmol l^{-1} NaCl) for fixation. After 3 min the ethanol was removed by pipetting after centrifugation (10,000*g*, 2 min) and FISH in liquid was performed according to ref. 59 with probes Arch915 (specific for Archaea)[60] and EUBmix (targeting most bacteria)[61] double-labelled with Fluos and Cy5, respectively[62]. Details on oligonucleotide probes are available at probeBase[63]. After FISH the biomass was dried onto CaF_2 slides, briefly dipped into ice-cold H_2O to wash off residual salts, air-dried with compressed air and transferred to a confocal LabRAM HR800 Raman microspectrometer (Horiba) equipped with a 50 mW 532 nm laser. Before Raman spectroscopy bright field and fluorescence images of biomass particles were acquired with the epifluorescence module of the Raman spectrometer. These images were imported into the LabSpec software package (version 5, Horiba) and cells for Raman analysis were chosen according to their positive FISH signals. Raman spectra of these cells were acquired with about 10% laser power. For most measurements, the pinhole was set to 200-µm diameter, which results together with the applied ×100 objective in an optical slice thickness of about 1.7 µm. The acquisition time was 150 s. The Raman spectra were recorded between ~120 and 1,800 cm^{-1} (with a spectral centre of 1,020 cm^{-1}), which covers most biologically significant signature peaks, including sulphur. Subsequently, CaF_2 peaks (at ~320 cm^{-1}) were subtracted, the spectra were baselined (polynom 4), mean normalized and transferred to a file format readable by Excel (Microsoft). Spectra of hybridized DSS cells could not be obtained as all cells were destroyed due to heating during Raman measurements. Solid standards, like iron phosphates and S_8 were measured directly on CaF_2 slides.

Transmission electron microscopy (TEM). TEM imaging was performed on the microbial mat sample from Black Sea. The mat was fixed in 4% formaldehyde in phosphate buffer (pH 7.4), washed and embedded in 2% agarose. The sample was then cut with a scalpel into small cubes (approximately 1 mm^3). Subsequently, the sample was embedded in EPON resin, contrasted by 1% aqueous osmium tetroxide and negatively stained with uranyl acetate using an automated microwave tissue processor (Leica Microsystems). The embedded sample was sectioned into ~70-nm sections using an ultramicrotome (Leica Microsystems). The sections were transferred on a formvar-coated copper grid, embedded in 2% methylcellulose and air-dried. Subsequently, the sections were carbon-coated and eventually analysed by electron energy-dispersive X-ray analysis (EDX) using transmission electron microscope (Tecnai G2 F20; FEI/Philips) equipped with an EDX detector.

NanoSIMS analysis of single cells. Image acquisition. All samples (immunogold-labelled thin sections and filter pieces containing hybridized cells from the disproportionation experiment) were analysed using a NanoSIMS 50L (Cameca). Secondary ions $^{12}C^-$, $^{13}C^-$, $^{12}C^{14}N^-$, $^{31}P^-$, $^{32}S^-$, $^{34}S^-$ and $^{12}C^-$, $^{12}C^{14}N^-$, $^{194}Pt^-$, $^{197}Au^-$ were recorded in subsequent runs, using 6 electron multipliers. To prevent charging, the samples were sputter-coated with platinum (gold-labelled sections) or gold-palladium (hybridized cells) before nanoSIMS analysis. All samples were pre-sputtered with a Cs^+ beam of ~500 pA to remove surface contaminations and to implant Cs^+ ions. For analysis, the samples were sputtered with a 0.3–1.3 pA Cs^+ primary ion beam focused into a spot of ~100-nm diameter that was scanned over the sample in a 256 × 256 pixel (gold-labelled sections) or 512 × 512 pixel (hybridized cells) raster with a counting time of 1 ms per pixel. The instrument was tuned for high mass resolution (5,000–6,000) of individual masses. The respective mass peaks were tuned directly on the sample ($^{12}C^-$, $^{13}C^-$, $^{12}C^{14}N^-$, $^{31}P^-$, $^{32}S^-$, $^{34}S^-$) or using a standard (platinum coating of the glass for $^{194}Pt^-$ and gold TEM grid for $^{197}Au^-$). For measurement of isotopes, t_0 samples from the respective experiments were analysed for natural abundance. Up to 150 planes were recorded for individual fields of view (15 µm × 15 µm).

Data processing. Ion-count images were processed using Look@NanoSIMS software[64]. For each field of view, the scanned planes were first aligned and accumulated. Subsequently, regions of interest (corresponding to individual cells) were defined by interactive thresholding[64], using images of $^{12}C^{14}N$, ^{31}P, and ^{32}S as masks. For each region of interest, $^{13}C/^{12}C$, $^{12}C^{14}N/^{12}C$, $^{31}P/^{12}C$, $^{32}S/^{12}C$, $^{32}S/^{12}C^{14}N$ and $(^{31}P/^{12}C)/(^{32}S/^{12}C)$ ratios were calculated. None of the ratios exhibited a significant trend with depth, which justified the use of accumulated ion images for the calculation of ratios in the defined regions of interest. All parameters for determining regions of interest, ratio calculations and further image processing are in detail described in ref. 64 and the software is freely available at http://www.microsen-wiki.net/lans.

On the basis of cell morphology, P, S and Au content, cells were automatically (based on a defined cut-off value of $^{31}P/^{32}S$) or manually (via visual inspection) identified as ANME or DSS (Supplementary Fig. 15b). The average doublings per day for ANME and DSS cells were calculated by subtracting the average $^{13}C/^{12}C$ ratio determined for the cells without label (that is, controls) from those incubated with added labelled DIC, and by subsequently dividing the difference with the ^{13}C-labelling percentage of DIC in the incubation medium divided by two and the incubation time (days).

Size calculation, biomass conversion and cellular activity calculations. For the methane carbon assimilation rates for ANME, a mean ($n = 10$) cell size was calculated assuming a cylindrical cell shape. The cellular length (1 µm) and width (0.5 µm) used for the size calculation was determined from TEM images and validated against nanoSIMS images. For the size-to-biomass conversion a calibration factor of 6.4 fmol C $µm^{-3}$ was used[56,65]. Subsequently, the cellular methane carbon assimilation rates were calculated as the $^{13}C/^{12}C$ enrichment of the ANME cells incubated with $^{13}CH_4$ multiplied by the average cellular biomass divided by ^{13}C-labelling % of the dissolved methane and incubation time (that is, 28 or 44 days).

Analysis of sulphur compounds. Sulphate was analysed on a 761 Compact ion chromatograph (Metrohm) with a Metrosep A SUPP 5 column. Carbonate buffer (3.2 mmol l^{-1} Na_2CO_3 and 1 mmol l^{-1} $NaHCO_3$) was used as eluent. The duration of a run was 14 min, with sulphate eluting at ~11.5 min.

Sulphite and thiosulphate in the medium were derivatized at room temperature in the dark with monobromobimane and analysed by HPLC according to the methods described in ref. 66.

Polysulphides were analysed by a modified method from ref. 20. Briefly, dissolved polysulphides were methylated using methyl trifluoromethanesulphonate (methyl triflate) to form methyl polysulphanes that can be separated and quantified using HPLC. Forty ml of anoxic methanol were vigorously stirred in a closed serum vial. Two liquids were rapidly injected into the stirred methanol from syringes: 10 ml of anoxic AOM biomass and/or medium followed immediately by 300 µl methyl triflate. The additional phosphate buffer used in ref. 20 was not used, because the medium was already strongly buffered. Eighty ml of sodium sulphate solution (375 mM) were added to the reaction mixture and transferred to a 250 ml separatory funnel. Subsequently, the solution was extracted with 2 × 1 ml *n*-dodecane. Elemental cyclosulphur compounds, such as S_6, S_7 and S_8, can also be extracted into the *n*-dodecane, but not in a quantitative manner[67].

The obtained extract was analysed by liquid chromatography (GP50 Gradient Pump, equipped with a C18 reverse phase column and a UVD340S Diode Array Detector; all by Dionex). Methanol was used as mobile phase and spectrophotometric detection was performed at 220 and 230 nm wavelengths. Detection limits were 600 nmol l^{-1}, 400 nmol l^{-1}, 300 nmol l^{-1}, 120 nmol l^{-1}, 100 nmol l^{-1} and 60 nmol l^{-1} for S_3^{2-}, S_4^{2-}, S_5^{2-}, S_6^{2-}, S_7^{2-} and S_8^{2-}, respectively. The identification of methylated polysulphides S_4^{2-} to S_6^{2-} was confirmed by gas chromatography-mass spectrometry (Trace GC-MS; ThermoFinnigan) according to ref. 49.

A standard series of polysulphides saturated with respect to elemental sulphur was prepared by dissolving excess elemental sulphur (S_8) in a solution containing ~10 mmol l^{-1} total dissolved sulphide in an anoxic solution buffered to pH 8.8 (50 mmol l^{-1} phosphate buffer). The resulting yellow polysulphide solution was left to stand overnight to equilibrate and was then methylated as described above. Equilibrium concentrations were calculated using the equilibrium constants from refs 49 and 68. The detection limit for total polysulphide zero-valent sulphur (based on resolved peaks of S_4^{2-}, S_5^{2-} and S_6^{2-}) was 3 μmol l^{-1}. The average relative standard deviation for the detection of inorganic polysulphide S^0 by the methyl triflate derivatization-based method is 8%[69].

It should be noted that the method for reaction of the methyl triflate with polysulphides is for solutions. The reaction depends on the very rapid methylation of the dianonic polysulphide compounds before they have the opportunity to disproportionate. The reaction of the methyl triflate with the biomass involves a solid phase. Thus, transport and diffusion of the methyl triflate to polysulphide species in the cell will be hindered. The determination of the precise speciation of polysulphides as in ref. 49 is therefore not possible. Moreover, methyl triflate is one of the most powerful methylating compounds known and is likely to react with other polysulphane-containing compounds or displace other capping groups on the ends of organic polylsulphane compounds. In spite of these caveats, the formation of the dimethyl polysulphane compounds provides an unequivocal indication of zero-valent sulphur in the biomass and medium.

Elemental sulphur was measured by methanol and/or chloroform extraction following the methods described in ref. 69 and modified for small volumes. We also measured zero-valent sulphur in biomass by reacting biomass samples preserved in zinc chloride solution (50% w/v) with sulphite solution to form thiosulphate. This is similar to the cyanolysis reaction for zero-valent sulphur described in ref. 69. To 0.65 ml of sample in a 2 ml capped Eppendorf tube 0.25 ml of 100 mmol l^{-1} sodium sulphite solution was added and the samples were allowed to react for 12 h (overnight) at 70 °C. Samples were then filtered through a 0.45-μm filter, diluted to 10 ml with water and analysed for thiosulphate using a 761 Compact ion chromatograph (Metrohm). The same column and the eluent were used as for the sulphate measurements. A pre-column was used that served as a zinc trap. The duration of a run was 22 min, with thiosulphate eluting at ~19 min.

Preparation of ^{35}S-labelled sulphide. ^{35}S-labelled sulphide was prepared by reduction of radiolabelled sulphate by the method from ref. 70 as modified by G. L. Arnold (personal communication). Briefly, ~5 MBq of ^{35}S-sulphate (18 GBq mol^{-1}; Hartmann Analytics) was added to 0.5 ml of 100 mmol l^{-1} sodium sulphate solution and gently dried (80 °C) in the bottom of a 250 ml round-bottom flask. The flask with dried sulphate salt and additional flask with boiling stones was connected to a reduction/distillation assembly consisting of a condenser, gas washing trap containing water and a 0.01 mol l^{-1} $AgNO_3$ trap. A reducing agent containing 163 ml of concentrated HCl, 100 ml of hydriodic acid, 50 ml of 50% hypophosphorous acid was prepared and boiled gently for about 1 h to remove sulphur contamination. Approximately 30 ml of the reducing agent was added to the reaction flask and gently boiled for 3 h. The collected Ag_2S was subsequently converted to ZnS using Cr II reduction method described below and the released sulphide was trapped in 10 ml of $ZnCl_2$ solution. Measured specific activity of the $Zn^{35}S$ suspension at the time of the experiment was 84.1 kBq μmol $^{-1}$ ZnS.

Incubation experiments with isotope-labelled substrates. Three different sets of incubation experiments were performed with the Isis enrichment culture under undisturbed AOM conditions.

(1) To test whether the biomass S originates from sulphate, the enrichment culture (12 ml liquid + biomass and 10 ml headspace) was incubated under AOM conditions (3 bar CH_4 overpressure) with $^{35}SO_4^{2-}$ tracer (~2.5 MBq; 18 GBq mol^{-1}; Hartmann Analytics) and 50 μmol l^{-1} sulphide in 22 ml Hungate tubes at room temperature on a shaker (40 r.p.m.) for up to 24 h. Subsamples (1 ml) were taken anoxically through the butyl rubber stopper with a needle after 1, 3, 6, 11 and 24 h and directly filtered through a 0.22-μm GTTP filter into zinc acetate solution (0.9 M) to stop the reaction and fix sulphide. The filter containing biomass flocks was immediately washed once with anoxic artificial seawater medium and twice with 20 ml of 1 M HCl solution to dissolve precipitated iron sulphides and subsequently analysed for ^{35}S by scintillation counting (scintillation cocktail: LumaSafeTM Plus; scintillation counter: 2900TR LSA, both Packard). At 0 and 24 h subsamples (0.3 ml culture in 50% $ZnCl_2$) were taken for total sulphide measurements. Sulphide was measured according to ref. 54.

This experiment was repeated and extended as follows: the Isis enrichment culture (10 ml liquid + biomass and 12 ml headspace) was incubated with ^{14}C-labelled methane (8.6 MBq; American Radiolabelled Chemicals), ^{13}C-labelled bicarbonate (50 atom percent ^{13}C), ^{34}S-labelled sulphate (50 atom percent ^{34}S; Icon Isotopes), ^{35}S-labelled sulphate (2.6 MBq) and 50 μmol l^{-1} sulphide in 22 ml Hungate tubes at room temperature for up to 144 h. At 0 and 24 h subsamples (0.3 ml) were taken for total sulphide measurements using colorimetry[54]. Two parallel subsamples (0.5 ml) were taken after 1, 3, 6, 11 and 24 h, which were directly filtered through 0.22-μm GTTP filters either into zinc acetate solution (0.9 M) to fix sulphide or into NaOH (0.6 M) to fix bicarbonate. One filter containing biomass flocks was immediately washed with anaerobic artificial seawater medium and 20 ml of 1 M HCl solution to dissolve precipitated iron sulphides and subsequently analysed by scintillation counting. The other biomass filter was transferred into 4% formaldehyde for subsequent nanoSIMS analysis.

(2) To test whether the biomass S originates from sulphide, ^{35}S-sulphide addition experiment was performed as follows: 5 ml of the $Zn^{35}S$ suspension was placed in a 50 ml serum vial and degassed with nitrogen. Subsequently, 1 ml of nitrogen-degassed phosphoric acid was added and the $Zn^{35}S$ dissolved, releasing $H_2{}^{35}S$ in the headspace. Approximately 2 ml of headspace gas containing $H_2{}^{35}S$ (~21 kBq) were then anoxically transferred with a syringe into a 22 ml Hungate tube with Isis enrichment culture (10 ml medium + biomass and 12 ml headspace) containing ~200 μmol l^{-1} sulphide. The Hungate tube was then supplemented with methane overpressure (3 bar) and incubated at room temperature in the dark on a shaker (40 r.p.m.) for up to 24 h. Subsamples (1 ml) were taken after 1, 3, 6, 11 and 24 h and directly filtered through a 0.22-μm GTTP filter into zinc acetate solution (0.9 M) to stop the reaction and fix sulphide. Total sulphide production was measured using colorimetry[54]. The filter containing biomass flocks was immediately washed once with anaerobic artificial seawater medium and twice with 20 ml of 1 M HCl solution to dissolve precipitated iron sulphides and subsequently analysed by scintillation counting. To determine the ^{35}S-sulphate production, 5 ml of the ZnAc-fixed sample was filtered through a 0.02-μm filter to remove ZnS and the flow-through was analysed by scintillation counting.

(3) To measure ^{13}C assimilation from methane and CO_2 by ANME and DSS, a following experiment was performed: Isis enrichment culture (100 ml medium + biomass and 56 ml headspace) was incubated in 156 ml serum bottles with either ^{13}C-labelled methane (50 atom % ^{13}C) or ^{13}C-labelled bicarbonate (4.6 atom % ^{13}C) in the dark at room temperature on a shaker (40 r.p.m.). In both bottles the sulphide concentrations were regularly monitored (according to ref. 52) and the medium was exchanged as soon as 2 mmol l^{-1} sulphide was produced to prevent accumulation of dissolved ^{13}C-intermediates and products (for example, $^{13}CO_2$ in the $^{13}CH_4$ incubations). At two time points (28 and 44 days) subsamples (0.5 ml) were taken for bulk ^{13}C measurements and for nanoSIMS analyses of single cells. For bulk ^{13}C measurements, 0.5 ml of the sample was filtered onto baked glass-fibre filters, washed and air-dried before analysis. Abundances of ^{13}C were measured using CO_2 released by flash combustion in excess oxygen at 1,050 °C in an automated elemental analyser (Thermo Flash EA, 1112 Series) coupled to a Deltaplus Advantage mass spectrometer (ThermoFinnigan). For nanoSIMS, biomass samples (0.5 ml) were fixed in 4% formaldehyde for 2 h at room temperature. Then, the supernatant containing medium salts and precipitates was removed and the biomass flocs were washed and stored in fresh 4% formaldehyde in 50 mmol l^{-1} phosphate buffer at 4 °C until further processing.

Determination of sulphate reduction and methane oxidation rates. In the first set of incubation experiments, radiolabelled reactants and products ($^{35}SO_4^{2-}$ and total reduced inorganic sulphur, respectively) were separated by cold chromium distillation[71].

In the incubation experiments with ^{14}C and ^{35}S, radiolabelled reactants ($^{14}CH_4$ and $^{35}SO_4^{2-}$) and products ($^{14}CO_2$ and total reduced inorganic sulphur) were separated as follows: ^{14}C-radiolabelled carbonate and reduced ^{35}S species were released from the NaOH-fixed sample by acidification with HCl and subsequent reducing Cr II addition. The mobilized species were separately trapped by bubbling through a series of chemical traps: (1) 7 ml of a 0.1 M, pH 4 citrate buffer; (2) a 5% zinc acetate trap adjusted to pH 6.2 with HCl; (3) a second zinc acetate trap with pH 2; (4) a trap containing 7 ml of Carbosorb E (a CO_2 absorber for scintillation counting; Perkin Elmer); and (5) a second Carbosorb E trap. The first trap (1) was designed to trap extraneous aerosols and drops from the acid solution, the second and third traps (2 and 3) were designed to catch ^{35}S, whereas $^{14}CO_2$, which passed through traps 2 and 3, was fully trapped in the final two traps (4 and 5). The separation method (for the [^{14}C]DIC and ^{35}S-H_2S) represents a novel method which is a combination and adaptation of two well-established methods. We have optimized pH in the traps, as well as the number of traps

required. The efficiency and recovery of the method was checked by tests with ^{35}S-sulphide and ^{14}C-bicarbonate standards.

The radioactivity of biomass, total dissolved reduced inorganic sulphur, dissolved inorganic carbon as well as dissolved sulphate was quantified by scintillation counting (scintillation cocktail: LumaSafeTM Plus; scintillation counter: 2900TR LSA, Packard). Sulphate reduction rates were determined as described in ref. 72. Methane oxidation rates were calculated as described in ref. 73. Due to the fact that the biomass from the third set of experiments contained both ^{14}C- and ^{35}S-label, methane carbon assimilation rates and biomass sulphur accumulation rates could not be directly measured. However, the individual contributions of ^{14}C and ^{35}S to the total recorded radioactivity could be determined due to their different half-lives of 5,730 years and 87 days, respectively. We recorded daily changes in the radioactivity of the biomass via regular scintillation counting over a period of ~3 weeks and based on the assumption that the activity of ^{14}C stays constant over the measuring period. We used following equation to calculate the ^{35}S and ^{14}C in the biomass

$$A_{^{14}\mathrm{C}} = \mathrm{TA}_t + A_{^{35}\mathrm{S}(t=0)}\mathrm{e}^{-\lambda t}$$

where $\mathrm{TA_t}$ = total measured activity at any time point, t = time in days, A = activity of ^{35}S or ^{14}C, λ = decay constant for ^{35}S.

Free energy calculations. The free energies of sulphate reduction to hydrodisulphide (equation (3) and Supplementary Fig. 12) and hydrodisulphide disproportionation reactions (equation (2)) were calculated using the following equation: $\Delta G = \Delta G^0 + R T \ln Q$ where ΔG^0 is the free energy of reaction at standard state calculated from the free energies of formation from the elements (G^0_f values taken from ref. 48, except for hydrodisulphide, which was obtained from ref. 49). R is the gas constant (8.314 J mol^{-1} K^{-1}), T is the temperature (K) and Q is the reaction quotient, $Q = ([HS_2^-]^4[HCO_3^-]^7[H_2O]^{11})/([CH_4]^7[SO_4^{2-}]^8)([H^+]^5)$ for equation (3) and $Q = ([HS^-]^7[SO_4^{2-}]^8)([H^+]^5)/([HS_2^-]^4[H_2O]^4)$ for equation (2).

Calculations of free energies of reactions (ΔG_{rxn}) were made using the concentrations and activity coefficients typical for the start of a batch enrichment culture listed in Supplementary Table 3 at 23 °C. Thermodynamic calculations for colder temperatures (5 to 14 °C) yield Gibbs free energies that are 10 to 15 kJ mol^{-1} less favourable (compared to room temperature) for all disproportionation reactions in Supplementary Table 2. Equilibrium speciation and activity coefficients were calculated using the software The Geochemist's Workbench V. 9.0 (Aqueous Solutions LLC). The exception was for hydrodisulphide that was calculated using a spreadsheet provided by A. Kamyshny, using the values from ref. 49 and assuming that the polysulphide system is saturated with respect to elemental sulphur. Activity coefficients were calculated using the extended Debye–Huckel model and an estimated ionic strength of 0.662 and at 25 °C. The activity of water was calculated to be 0.982. The ionic strength of this seawater medium is slightly above the value of 0.5 to which the extended Debye–Huckel model is deemed to be accurate. The Harvie–Møller–Weare (HMW) model using virial coefficients is more accurate, but the database does not contain virial coefficients for reduced sulphur components. For comparison, calculation of the free sulphate and bicarbonate anion activities is about 10% greater using the HMW thermodynamic database. Given the stoichiometries of the reactions 1 and 2 (Supplementary Table 4), these differences nearly cancel out one another.

48. Stumm, W. & Morgan, J. J. in *Aquatic Chemistry: Chemical Equilibria and Rates in Natural Waters* 3rd edn, 990–1003 (Wiley-Interscience, 1996).
49. Kamyshny, A., Goifma, A., Gun, J., Rizkov, D. & Lev, O. Equilibrium distribution of polysulfide ions in aqueous solutions at 25°C: a new approach for the study of polysulfide's equilibrium. *Environ. Sci. Technol.* **38,** 6633–6644 (2004).
50. Mastalerz, V., de Lange, G. J., Dählmann, A. & Feseker, T. Active venting at the Isis mud volcano, offshore Egypt: origin and migration of hydrocarbons. *Chem. Geol.* **246,** 87–106 (2007).
51. Widdel, F. & Bak, F. in *The Prokaryotes* (eds. Balows A. T. *et al.*) Vol. 4, 3352–3378 (Springer, 1992).
52. Cord-Ruwisch, R. A quick method for the determination of dissolved and precipitated sulfides in cultures of sulfate-reducing bacteria. *J. Microbiol. Methods* **4,** 33–36 (1985).
53. Saleh, A. M., Macpherson, R. & Miller, J. D. A. The effect of inhibitors on sulphate reducing bacteria: a compilation. *J. Appl. Bacteriol.* **27,** 281–293 (1964).
54. Cline, J. D. Spectrophotometric determination of hydrogen sulfide in natural waters. *Limnol. Oceanogr.* **14,** 454–458 (1969).
55. Steudel, R., Göbel, T. & Holdt, G. The molecular composition of hydrophilic sulfur sols prepared by acid decomposition of thiosulfate. *Z. Naturforsch.* **43b,** 203–218 (1988).
56. Musat, N. *et al.* A single-cell view on the ecophysiology of anaerobic phototrophic bacteria. *Proc. Natl Acad. Sci. USA* **105,** 17861–17866 (2008).
57. Tokuyasu, K. T. Technique for ultracryotomy of cell suspensions and tissues. *J. Cell Biol.* **57,** 551–565 (1973).
58. Milucka, J., Widdel, F. & Shima, S. Immunological detection of enzymes for sulfate reduction in anaerobic methane-oxidizing consortia. *Environ. Microbiol.* http://dx.doi.org/10.1111/1462-2920.12003 (28 September 2012).
59. Huang, W. E. *et al.* Raman-FISH: combining stable-isotope Raman spectroscopy and fluorescence *in situ* hybridization for the single cell analysis of identity and function. *Environ. Microbiol.* **9,** 1878–1889 (2007).
60. Stahl, D. A. & Amann, R. in *Nucleic Acid Techniques in Bacterial Systematics* (eds. Stackebrandt, E. & Goodfellow, M.) 205–248 (John Wiley, 1991).
61. Daims, H., Brühl, A., Amann, R., Schleifer, K. H. & Wagner, M. Probe EUB338 is insufficient for the detection of all Bacteria: development and evaluation of a more comprehensive probe set. *Syst. Appl. Microbiol.* **22,** 434–444 (1999).
62. Stoecker, K., Dorninger, C., Daims, H. & Wagner, M. Double-labeling of oligonucleotide probes for fluorescence *in situ* hybridization (DOPE-FISH) improves signal intensity and increases rRNA accessibility. *Appl. Environ. Microbiol.* **76,** 922–926 (2010).
63. Loy, A., Maixner, F., Wagner, M. & Horn, M. probeBase—an online resource for rRNA-targeted oligonucleotide probes: new features 2007. *Nucleic Acids Res.* **35,** D800–D804 (2007).
64. Polerecky, L. *et al.* Look@NanoSIMS – a tool for the analysis of nanoSIMS data in environmental microbiology, *Environ. Microbiol.* **14,** 1009–1023 (2012).
65. Ploug, H. *et al.* Carbon and nitrogen fluxes associated with the cyanobacterium *Aphanizomenon* sp. in the Baltic Sea. *ISME J.* **4,** 1215–1223 (2010).
66. Zopfi, J., Ferdelman, T. G. & Fossing, H. in *Sulfur Biogeochemistry - Past and Present* (eds. Amend, J., Edwards, K. J. & Lyons, T. W.) Vol. 379, 97–116 (The Geological Society of America Special Paper, 2004).
67. Kamyshny, A. Solubility of cyclooctasulfur in pure water and sea water at different temperatures. *Geochim. Cosmochim. Acta* **73,** 6022–6028 (2009).
68. Kamyshny, A., Gun, J., Rizkov, D., Voitsekovski, T. & Lev, O. Equilibrium distributions of polysulfide ions in aqueous solutions at different temperatures by rapid phase derivitization. *Environ. Sci. Technol.* **41,** 2395–2400 (2007).
69. Kamyshny, A., Borkenstein, C. G. & Ferdelman, T. G. Protocol for quantitative detection of elemental sulfur and polysulfide zero-valent sulfur distribution in natural aquatic samples. *Geostand. Geoanal. Res.* **33,** 415–435 (2009).
70. Thode, H. G., Monster, J. & Dunford, H. B. Sulphur isotope geochemistry. *Geochim. Cosmochim. Acta* **25,** 159–174 (1961).
71. Kallmeyer, J., Ferdelman, T. G., Weber, A., Fossing, H. & Jørgensen, B. B. A cold chromium distillation procedure for radiolabeled sulfide applied to sulfate reduction measurements. *Limnol. Oceanogr. Methods* **2,** 171–180 (2004).
72. Jørgensen, B. B. & Fenchel, T. Sulfur cycle of a marine sediment model system. *Mar. Biol.* **24,** 189–201 (1974).
73. Treude, T., Boetius, A., Knittel, K., Wallmann, K. & Jørgensen, B. B. Anaerobic oxidation of methane above gas hydrates at Hydrate Ridge, NE Pacific Ocean. *Mar. Ecol. Prog. Ser.* **264,** 1–14 (2003).